

SUPPORTING INFORMATION

Synergistic effect of adsorption coupled catalysis based on graphene-supported MOF hybrid aerogel for promoted removal of dyes

Yinjia Wan§, Jianzhi Wang§, Fei Huang, Yanan Xue, Ning Cai, Jie Liu, Weimin Chen, Faquan Yu*

Key Laboratory for Green Chemical Process of Ministry of Education

Hubei Key Laboratory for Novel Reactor and Green Chemistry Technology

School of Chemical Engineering and Pharmacy,

Wuhan Institute of Technology, Wuhan 430073, China

*Corresponding author: Faquan Yu (fyu@wit.edu.cn, fyuwucn@gmail.com)

Simulation Process

To express the coupling effect of absorption and catalysis, we hypothesized the equilibrium concentration only when absorption process happens would be reduced by the catalysis process in the mode of catalysis kinetics rate. In terms of the absorption mode discussed above, pseudo-second-order adsorption was adopted here. The catalytic degradation process was expressed in pseudo-first-order way in light of the data in Fig S5.

First, Q_t and Q_e were transformed into C_t and C_e as follows:

$$Q_t = \frac{(C_0 - C_t) \cdot V}{m}$$

$$Q_e = \frac{(C_0 - C_e) \cdot V}{m}$$

The pseudo-second-order adsorption could be expressed as follows:

$$\frac{t}{C_0 - C_t} = \frac{m}{k_a V (C_0 - C_e)^2} + \frac{t}{C_0 - C_e} \quad (1)$$

The pseudo-first-order degradation model was expressed as follows:

$$C_e = C_{e0} e^{-k_c t} \quad (2)$$

Substitute equation (2) for (1):

$$\frac{t}{C_0 - C_t} = \frac{m}{k_a V (C_0 - C_{e0} e^{-k_c t})^2} + \frac{t}{C_0 - C_{e0} e^{-k_c t}}$$

Therefore:

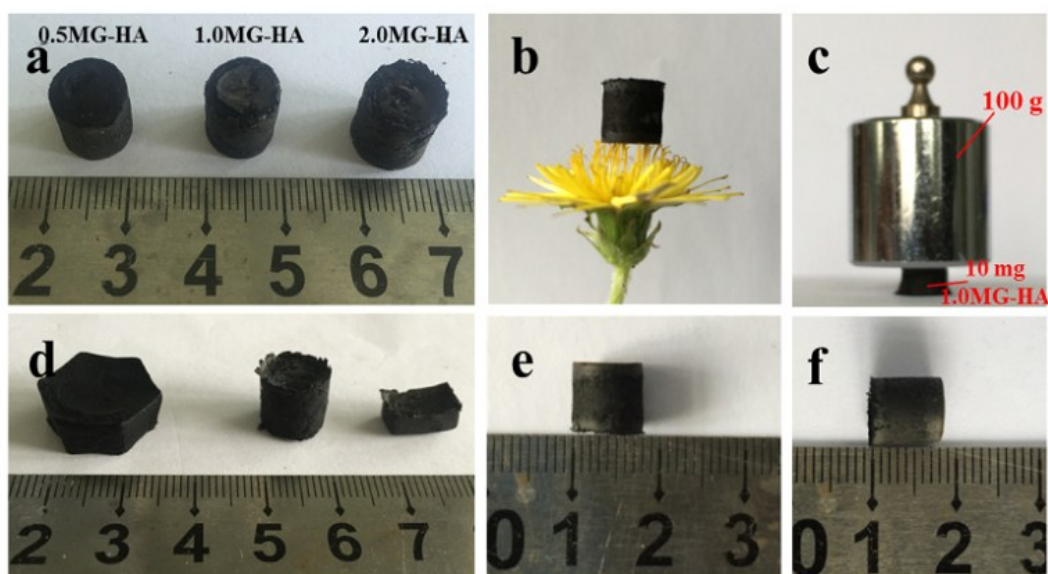
$$\frac{C_t}{C_0} = 1 - \frac{t}{\frac{m C_0}{k_a V (C_0 - C_{e0} e^{-k_c t})^2} + \frac{t C_0}{C_0 - C_{e0} e^{-k_c t}}}$$

where Q_t (mg g⁻¹) is the adsorption amount at absorption time t , Q_e (mg g⁻¹) is the equilibrium adsorption amount, C_0 (mg L⁻¹) is the initial concentration of dye, C_t (mg L⁻¹) is the concentration of dye at time t , C_e (mg L⁻¹) is the equilibrium concentration at the time t after degradation happened, C_{e0} (mg L⁻¹) is the equilibrium concentration without degradation process, k_a (g mg⁻¹ min⁻¹) is the adsorption pseudo-

second-order rate constant, k_c (min^{-1}) is the catalytic degradation pseudo-first-order rate constant. m (g) is the mass of adsorbent, and V (L) is the volume of the solution, t (min) is the reaction time.

UV-vis detection of Desorbed solution

By mixing 10 mg of 1.0MG-HA with 20 mL of 200 mg L^{-1} MB aqueous solutions at 30 °C at 130 rpm in a shaking bath, the adsorbent was collected. Then 20 ml ethanol was added. The suspension was shaken at 130 rpm for 8 h in order to release the pollutants. The supernatant was checked by UV-Vis absorbance from 500 to 750nm. As comparison, 10 mg of 1.0MG-HA was added into 20 mL of 200 mg L^{-1} MB aqueous solutions containing 100 μl H_2O_2 for achievement of absorption and degradation processes. All the processes were run as above. The results were shown



in Figure S3.

Figure S1. The digital photograph of (a) appearance of MG-HA in different preparation formulations, (b, c) intuitive display of ultralight density and strong mechanical strength, (d) shapes prepared in different moulds, and (e, f) typical sizes of as prepared three-dimensional 1.0MG-HA.

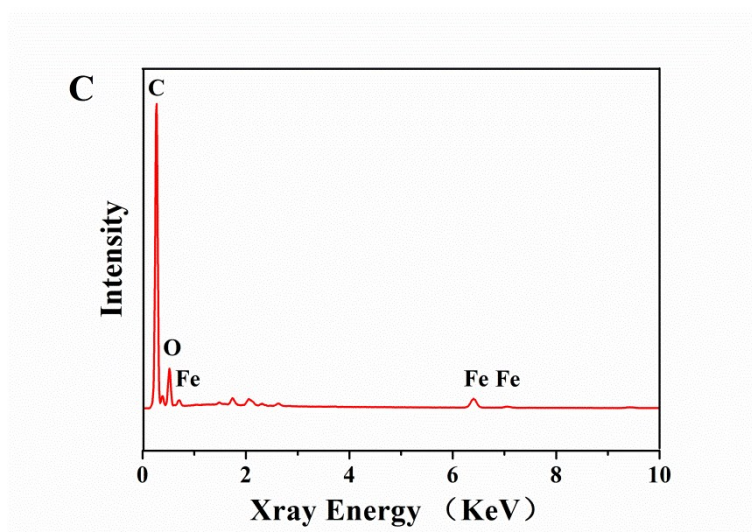
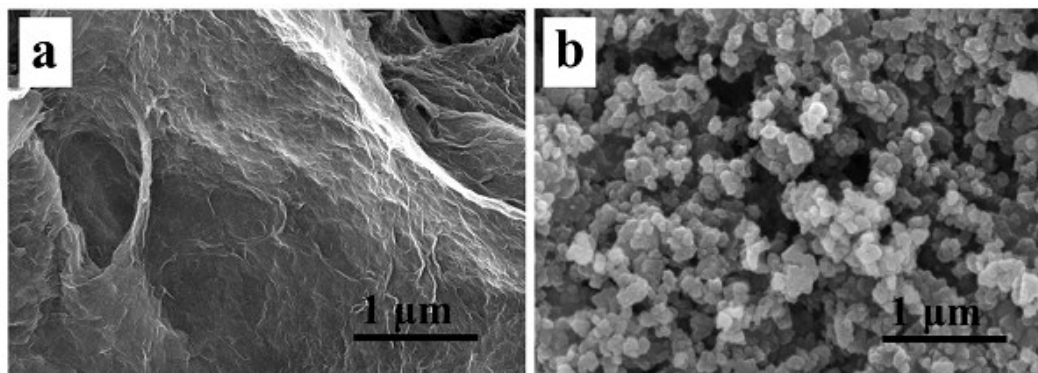


Figure S2. (a) SEM image of GA, (b) MIL-100(Fe) and (c) EDX of 1.0MG-HA

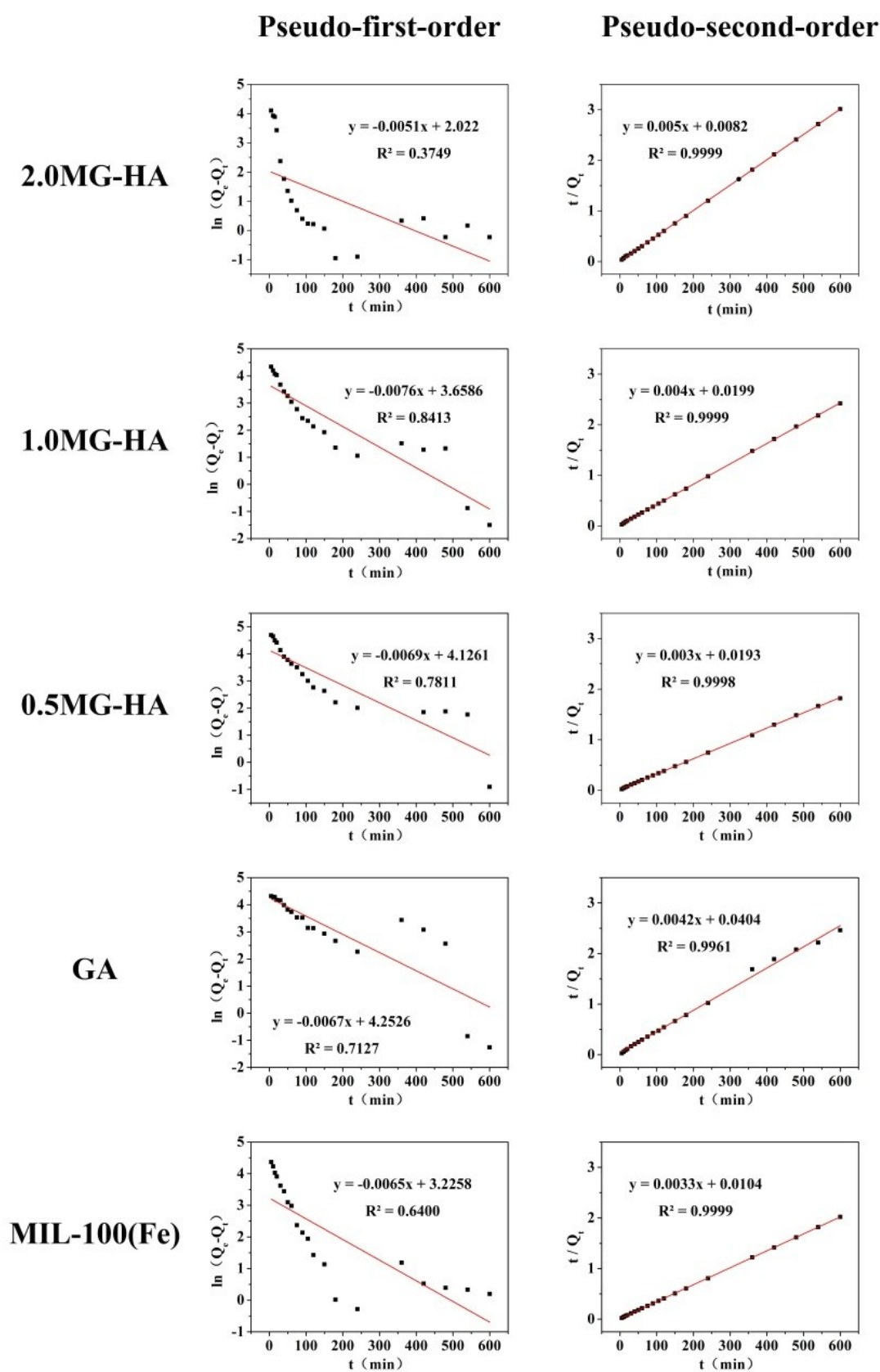


Figure S3. Pseudo-first-order and Pseudo-second-order kinetic plots for MB adsorption on MG-HA, MIL-100(Fe) and GA

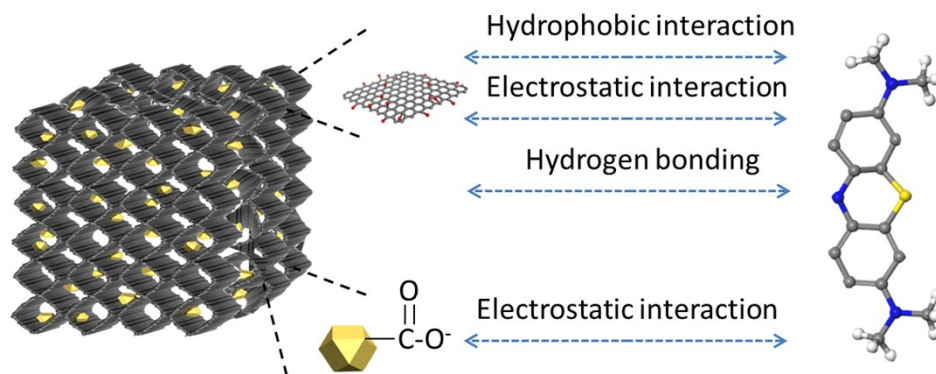


Figure S4. Schematic diagram of the possible adsorption mechanism of MG-HA to MB.

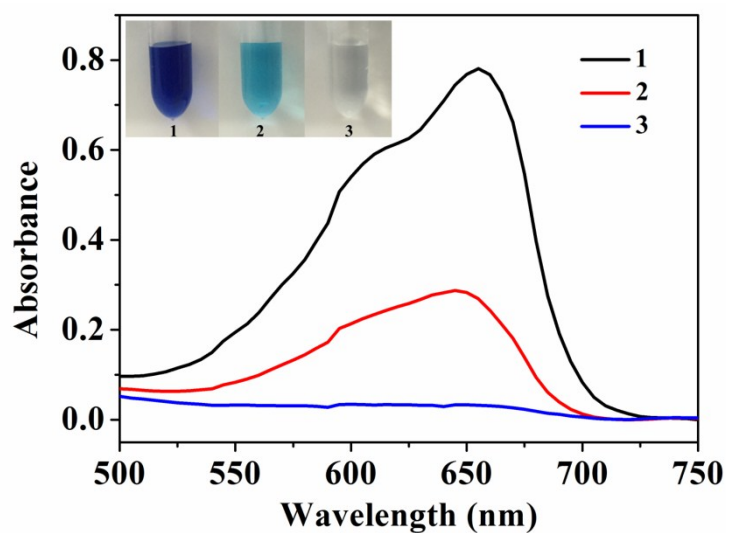


Figure S5. UV-Vis absorbance spectra of (1) the initial MB solution, (2) the desorbed solution from only absorption effect and (3) the desorbed solution from absorption/catalysis effect. The inset is the digital photo of the corresponding solutions.

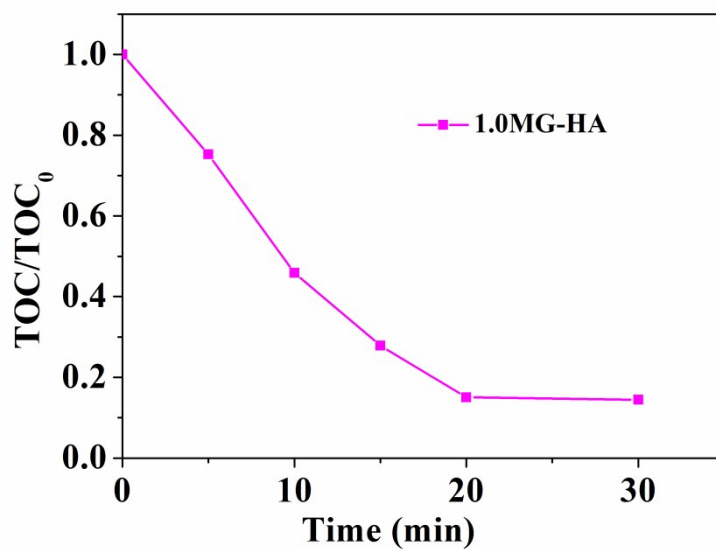


Figure S6. Mineralization of MB (200 mg L⁻¹) by the “1.0MG-HA+H₂O₂” system.

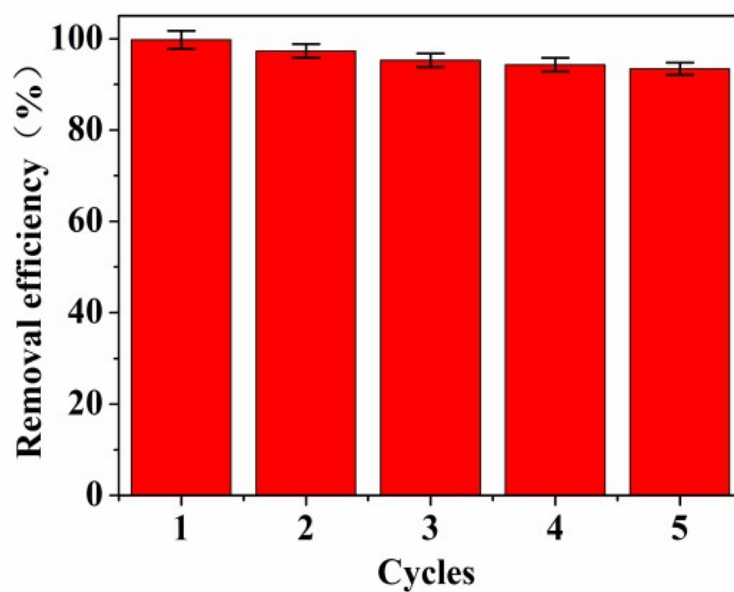


Figure S7. Removal efficiency of MB in 5 successive cycles of applications by 1.0MG-HA adsorption/catalyst (initial MB concentration 200 mg L⁻¹).

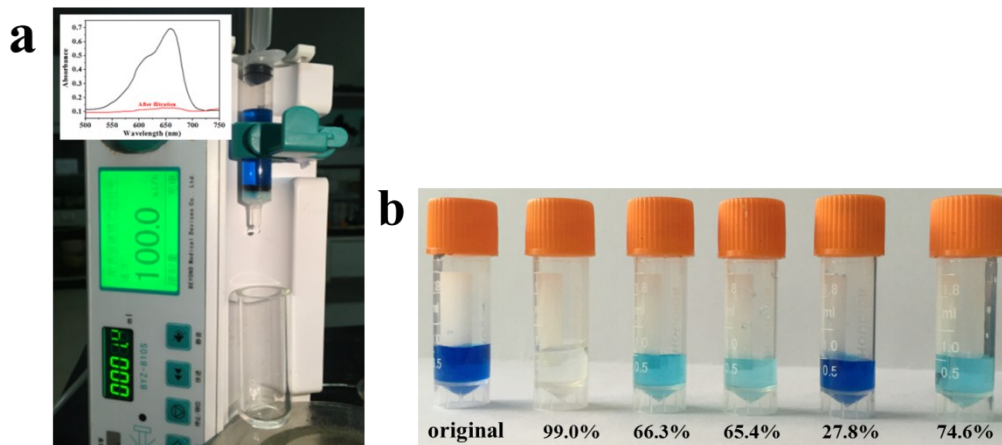


Figure S8. (a) syringe filter for the separation of MB and (b) comparison of separation activity among different absorbents (from left to right: blank, 1.0MG-HA, cotton, GA, MIL-100(Fe) and activated carbon). The data shown underneath the vials represent the removal efficiency.

Table S1 Adsorption kinetic parameters of MB on MG-HA, MIL-100(Fe) and GA

Sample	Pseudo-first-order			Pseudo-second-order		
	k_a (min^{-1})	Q_e (mg g^{-1})	R^2	k_a ($\text{g mg}^{-1} \text{min}^{-1}$)	Q_e (mg g^{-1})	R^2
2.0MG-HA	0.0309	37.95	0.3749	0.0030	200.00	0.9999
1.0MG-HA	0.0069	61.93	0.7811	0.0005	333.33	0.9998
0.5MG-HA	0.0076	38.81	0.8413	0.0007	250.00	0.9999
GA	0.0067	70.29	0.7127	0.0004	238.00	0.9961
MIL-100(Fe)	0.0065	25.17	0.6400	0.0010	303.03	0.9999

Table S2 The adsorption/catalysis constants under four different conditions

Condition	k_c (min^{-1})	k_a ($\text{g mg}^{-1} \text{min}^{-1}$)	C_0 (mg L^{-1})	C_{e0} (mg L^{-1})
H_2O_2	0	-	200	199.0
1.0MG-HA	0	0.0007	200	43.75
① 1.0MG-HA	0	0.0007	200	43.75
② H_2O_2	0.1665			
1.0MG-HA+ H_2O_2	0.1665	0.0007	200	43.75